

Exact solution and surface critical behaviour of an $O(n)$ model on the honeycomb lattice

This article has been downloaded from IOPscience. Please scroll down to see the full text article.

1993 J. Phys. A: Math. Gen. 26 L729

(<http://iopscience.iop.org/0305-4470/26/16/004>)

View [the table of contents for this issue](#), or go to the [journal homepage](#) for more

Download details:

IP Address: 171.66.16.68

The article was downloaded on 01/06/2010 at 19:24

Please note that [terms and conditions apply](#).

LETTER TO THE EDITOR

Exact solution and surface critical behaviour of an $O(n)$ model on the honeycomb lattice

M T Batchelor† and J Suzuki‡

† Mathematics Department, School of Mathematical Sciences, Australian National University, Canberra ACT 0200, Australia

‡ Institute of Physics, College of Arts and Sciences, University of Tokyo, Komaba 3-8-1, Meguro-ku, Tokyo, Japan

Received 21 May 1993

Abstract. We obtain the exact Bethe ansatz solution of an $O(n)$ model on the honeycomb lattice with open boundaries across a finite strip. Several quantities relevant to the surface critical behaviour of the $O(n)$ model are derived from this solution. The exact surface critical exponents are in agreement with those obtained by Cardy and by Duplantier and Saleur based on conformal invariance arguments.

The representation of polymers in terms of the $n = 0$ limit of the n -vector or $O(n)$ model (see, e.g. [1]), along with Coulomb gas methods, conformal invariance arguments and exact solutions, has led to the discovery of many new exact results for the configurational statistics of two-dimensional polymers (for reviews, see e.g. [2–4]). These include infinite families of exact critical exponents describing the correlation of polymers in both the *dilute* and *dense* phases. These results have also been extended by Cardy [5] and by Duplantier and Saleur [6] to describe *surface* critical behaviour (for a recent review covering also numerical results, see [7]).

In this letter we give an exact Bethe ansatz solution of an $O(n)$ model on the honeycomb lattice with *open* boundaries. We use this exact solution to derive, via Cardy's amplitude-exponent relation for finite-size scaling in open strips [8], the critical exponents characterizing the surface critical behaviour.

Our starting point is the high-temperature expansion of the partition function of the $O(n)$ model of Domany *et al* [9] which can be written as a sum over all configurations of closed and non-intersecting loops

$$Z = \sum t^{N-b} n^P \quad (1)$$

where N is the total number of lattice sites, b is the total number of bonds covered, P is the number of loops and t is the fugacity of an empty site. For this model Nienhuis [10] obtained the criticality condition

$$t^2 = 2 + \sqrt{2 - n}. \quad (2)$$

Here $n = -2 \cos \pi g$, where g is the Coulomb gas coupling constant, with $g \in [1, 2]$ in the high-temperature (critical) phase and $g \in [0, 1]$ in the low-temperature (dense) phase.

Now Baxter [11] also obtained (2) as a condition for solvability of the underlying three-state vertex model, i.e. as a condition for the diagonalization of the corresponding row-to-row transfer matrix by means of the coordinate Bethe ansatz. More generally this vertex model is a limit of the Izergin–Korepin model [12] (see, e.g. [13]). The row-to-row transfer matrix of this latter model has been diagonalized by means of the so-called analytic ansatz [14, 15], the algebraic Bethe ansatz [16] and the coordinate Bethe ansatz [17].

In order to make the above loop model equivalent to a vertex model, each loop carries an orientation as shown in figure 1(a). Each left (right) turn is then associated with a weight $e^{i\alpha}$ ($e^{-i\alpha}$), where $n = 2 \cos 6\alpha$. To derive the Bethe ansatz solution of this model we begin by noting that the honeycomb lattice can be transformed into the square lattice (see figure 1 and also [13]). On the square lattice, the model can be regarded as a 17-vertex model, with allowed vertices and corresponding weights as shown in figure 2. Also shown are the six possible boundary configurations. Following Baxter [11], we then interpret the vertex model as a line model (see also figure 2). The number of lines in a given row of diagonal bonds is a conserved quantity and the line model is amenable to the coordinate Bethe ansatz. To obtain the solution we employ a similar approach to that adopted by Owczarek and Baxter [18] in their treatment of the six-vertex model.

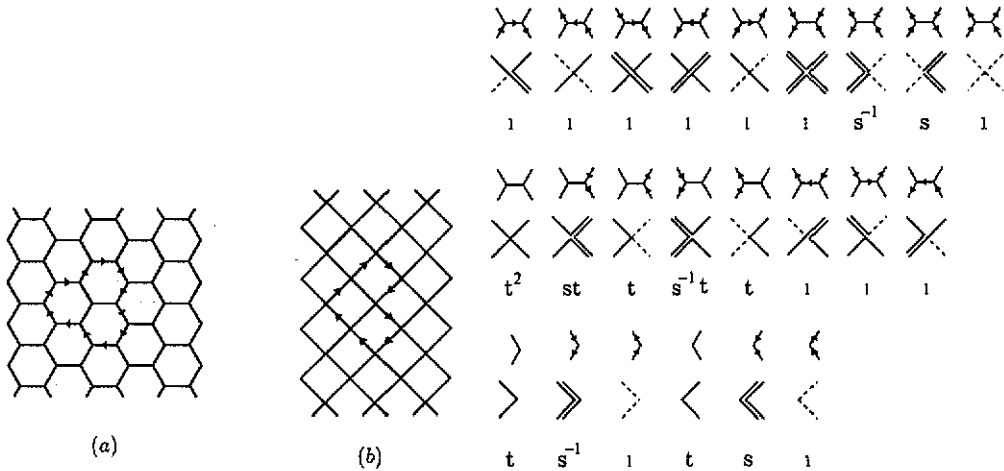


Figure 1. Finite strip of width $L = 6$ on (a) the honeycomb lattice and (b) the equivalent square lattice.

Figure 2. Allowed states on the honeycomb lattice (above) and their corresponding line representations on the square lattice (below). The corresponding vertex weights are also indicated. The last set of diagrams correspond to boundary configurations. The weights are given by $s = -e^{-i4\lambda}$ and $t = 2 \cos \lambda$.

From figure 1, we note that there are two types of transfer matrix, say T_1 and T_2 . Thus we must solve two coupled eigenvalue equations,

$$T_1 F = \Lambda G \quad T_2 G = \Lambda F. \tag{3}$$

Letting x_1, \dots, x_ℓ denote the position of the ℓ lines in a row, we adopt the following ansätze for the eigenfunctions,

$$F(x_1, \dots, x_\ell) = \sum \mathcal{A}(k_{p_1}, \dots, k_{p_\ell}) f(k_{p_1}, x_1) \times \dots \times f(k_{p_\ell}, x_\ell) \tag{4}$$

$$G(x_1, \dots, x_\ell) = \sum \mathcal{A}(k_{p_1}, \dots, k_{p_\ell}) g(k_{p_1}, x_1) \times \dots \times g(k_{p_\ell}, x_\ell)$$

in which the 'one-body' wavefunctions assume the form

$$f(k, x) = \begin{cases} A_e e^{ikx} & x \text{ even} \\ A_o e^{ikx} & x \text{ odd} \end{cases} \quad g(k, x) = \begin{cases} B_e e^{ikx} & x \text{ even} \\ B_o e^{ikx} & x \text{ odd} \end{cases} \quad (5)$$

and summations are taken over all permutations and all negations. As for the row-to-row transfer matrix case [11], we introduce two types of 'one body' wavefunction for doubly occupied states. The eigen equations determine the relation between the coefficients of all 'one body' wavefunctions and the consistency equations among the $\mathcal{A}(k_{p_1}, \dots, k_{p_t})$.

Omitting the details of the derivation, we find that the eigenvalues of the transfer matrix product $T_1 T_2$ are given by

$$\Lambda^2 = \prod_{j=1}^{\ell} \frac{\sinh(u_j + i3\lambda/2) \sinh(u_j - i3\lambda/2)}{\sinh(u_j + i\lambda/2) \sinh(u_j - i\lambda/2)} \quad (6)$$

where the u_j follow as roots of the Bethe ansatz equations

$$\begin{aligned} & \left[\frac{\sinh(u_j - i\lambda/2)}{\sinh(u_j + i\lambda/2)} \right]^2 \left[\frac{\sinh(u_j - i\lambda/2) \sinh(u_j - i3\lambda/2)}{\sinh(u_j + i\lambda/2) \sinh(u_j + i3\lambda/2)} \right]^L \\ &= \prod_{k \neq j}^{\ell} \frac{\sinh(u_j - u_k + i\lambda) \sinh(u_j + u_k + i\lambda) \sinh(u_j - u_k - i2\lambda) \sinh(u_j + u_k - i2\lambda)}{\sinh(u_j - u_k - i\lambda) \sinh(u_j + u_k - i\lambda) \sinh(u_j - u_k + i2\lambda) \sinh(u_j + u_k + i2\lambda)}. \end{aligned} \quad (7)$$

Here L is the width of the strip (e.g. $L = 6$ in figure 1(b)). The total number of lines ℓ label the sectors of $T_1 T_2$ with $\ell = L$ for the largest eigenvalue Λ_0 . The parameter λ is related to n and t via

$$n = -2 \cos 4\lambda \quad t = 2 \cos \lambda. \quad (8)$$

The relationships with other parametrizations of n are given by $4\lambda + \pi g = 2\pi$ and $\lambda = (\pi - \theta)/2$ [11].

We now proceed to derive the critical behaviour from the Bethe ansatz solution. As the approach is quite standard, we simply sketch the details. Detailed working of similar calculations for the same $O(n)$ model with *periodic* boundaries can be found in [19] and [20]. We first consider the thermodynamic limit $L \rightarrow \infty$. We define the Fourier transformation of a function $a(u)$ by

$$\bar{a}[x] = \frac{1}{2\pi} \int_{-\infty}^{\infty} a(u) e^{ixu} du \quad a(u) = \int_{-\infty}^{\infty} \bar{a}[x] e^{-ixu} dx. \quad (9)$$

The explicit form of the root density for Λ_0 follows as

$$\bar{\rho}_{\infty}[x] = \frac{2 \cosh \frac{1}{2} \lambda x}{2 \cosh \lambda x - 1}. \quad (10)$$

The free energy per vertex, f_{∞} , is then

$$\begin{aligned} f_{\infty} &= - \lim_{L \rightarrow \infty} \log \Lambda_0^2 \\ &= - \int_{-\infty}^{\infty} \frac{\sinh(\frac{1}{2} \pi - \lambda)x \sinh \lambda x}{x \sinh \frac{1}{2} \pi x (2 \cosh \lambda x - 1)} dx. \end{aligned} \quad (11)$$

This expression coincides with the previous result [11].

For periodic boundaries, there is a *cusp* in the free energy at $\lambda_0 \simeq 1.357$, with a different expression for the free energy in the region $\lambda_0 < \lambda < \pi/2$ [11, 21]. However, for open boundaries there is no cusp and the result (11) holds over the whole region $0 \leq \lambda \leq \pi/2$. This is a clear example of boundary effects modifying the bulk behaviour. In the present case, the difference is due to entropic effects, i.e. the number of possible configurations is suppressed by the presence of 'walls'. Indeed, at $\lambda = \pi/2$ it can be readily shown that for open boundaries the partition function is given by $Z = 2^L$ and thus $f_\infty = 0$, while for periodic boundaries, $f_\infty = -0.37912\dots$ [11].

In the absence of any spectral parameter, the finite-size corrections for this model can nevertheless be readily obtained via the root-density method developed by de Vega and Woynarovich *et al* (see, e.g. [22, 20] and references therein). We begin with the function

$$2\pi z_L(u) = \phi\left(u, \frac{\lambda}{2}\right) + \phi\left(u, \frac{3\lambda}{2}\right) - \frac{1}{L} \sum_{k=-\ell}^{\ell} [\phi(u - u_k, 2\lambda) - \phi(u - u_k, \lambda)] + \frac{1}{L} \Phi(u) \quad (12)$$

where

$$\phi(u, \lambda) = 2 \tan^{-1}(\cot \lambda \tanh u) \quad (13)$$

and

$$\Phi(u) = 2\phi(u, \frac{1}{2}\lambda) + \phi(u, 2\lambda) - \phi(u, \lambda) + \phi(2u, 2\lambda) - \phi(2u, \lambda). \quad (14)$$

In defining the function $z_L(u)$ we have used the symmetry of the root distribution under $u \rightarrow -u$. Its derivative, $\rho_L(u)$, satisfies the integral equation

$$\rho_L(u) - \rho_\infty(u) = \frac{1}{4\pi^2 L} \int K_1(u - u') \Phi(u') du' + \frac{1}{2\pi} \int K_2(u - u') S_L(u') du' \quad (15)$$

where

$$S_L(u) = \frac{1}{L} \sum_{j=-\ell}^{\ell} \delta(u - u_j) - \rho_L(u) \quad (16)$$

$$\bar{K}_1[x] = \frac{\sinh \frac{1}{2}\pi x}{(2 \cosh \lambda x - 1) \sinh(\frac{1}{2}\pi - \lambda)x} \quad (17a)$$

$$\bar{K}_2[x] = \frac{2 \cosh \frac{1}{2}(\pi - 3\lambda)x \sinh \frac{1}{2}\lambda x}{(2 \cosh \lambda x - 1) \sinh(\frac{1}{2}\pi - \lambda)x} \quad (17b)$$

The finite-size correction to the free energy is given by

$$f_L - f_\infty = -\frac{1}{2L} \log \left(\frac{1 - \cos \lambda}{1 - \cos 3\lambda} \right) - \frac{1}{8L\pi^2} \int K_1(u - u') \Phi(u') e_1(u) du du' - \frac{1}{2} \int S_L(u) e_2(u) du. \quad (18)$$

where

$$\bar{e}_1[x] = \frac{2 \sinh(\frac{1}{2}\pi - \lambda)x}{\sinh \frac{1}{2}\pi x} \quad \bar{e}_2[x] = \frac{\sinh \frac{1}{2}\lambda x}{x(2 \cosh \lambda x - 1)}. \quad (19)$$

The first and the second terms in (18) contribute to the surface free energy f_s . Explicitly, we find

$$f_s = -\frac{1}{2} \log \left(\frac{1 - \cos \lambda}{1 - \cos 3\lambda} \right) - 4 \int_{-\infty}^{\infty} \frac{\sinh \frac{1}{2}\lambda x \cosh \frac{1}{4}\lambda x \cosh \frac{1}{4}(\pi - 2\lambda)x \sinh \frac{1}{4}(\pi - 3\lambda)x (2 \cosh \frac{1}{2}\lambda x - 1)}{x \sinh \frac{1}{2}\pi x (2 \cosh \lambda x - 1)} dx. \quad (20)$$

The surface free energy is shown as a function of λ in figure 3. We note that f_s vanishes precisely at the $n = 0$ dilute polymer point ($\lambda = \pi/8$)†, whereas $f_s > 0$ at the $n = 0$ dense polymer point ($\lambda = 3\pi/8$), i.e. the dense polymers feel a repulsion from the boundary.

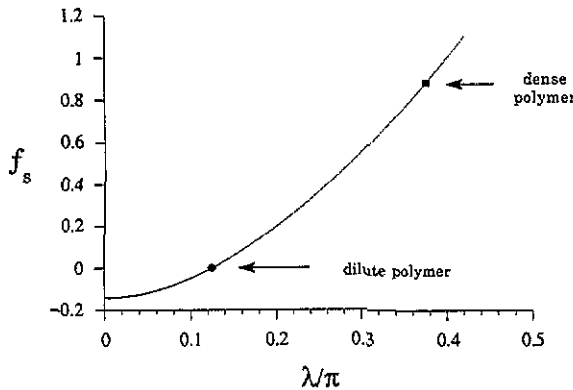


Figure 3. Surface free energy of the honeycomb $O(n)$ model as a function of λ .

In order to find the amplitudes of the $O(1/L^2)$ contributions, we solve equation (15), under the sum rule

$$\int_{-\infty}^{\infty} \rho_L(u) du = 2 + \frac{2(\hat{\ell} + 1)}{L} \left(1 - \frac{2\lambda}{\pi} \right) \quad (21)$$

where $\hat{\ell} = L - \ell$ is a more convenient sector label. Employing the standard argument based on the Wiener-Hopf method, we find

$$f_L(\hat{\ell}) = f_\infty + \frac{f_s}{L} - \frac{\pi \zeta c_{\hat{\ell}}}{24L^2} \quad (22)$$

where $f_L(\hat{\ell})$ is the lowest free energy in sector $\hat{\ell}$, ζ (a scale factor) = $\pi/3$, and

$$c_{\hat{\ell}} = 1 - \frac{3}{\pi(\pi - 2\lambda)} [(\pi - 4\lambda) + 2\hat{\ell}(\pi - 2\lambda)]^2. \quad (23)$$

† Moreover, we observe that all finite-size corrections to the free energy vanish at this point, with $\Lambda_0 = (2 + \sqrt{2})^L$, where $\mu = \sqrt{2} + \sqrt{2}$ is the connective constant for self-avoiding walks. A similar point exists at $n = 1$ in the low-temperature phase ($\lambda = \pi/3$) where $\Lambda_0 = 2^{L-1}$.

It thus follows [23] that the central charge is given by $c = c_0$, in agreement with the earlier identifications. The scaling dimensions of the theory follow from the amplitude-exponent relation [8]

$$\log \frac{\Lambda_0}{\Lambda_{\hat{\ell}}} \sim \frac{\pi \zeta x_{\hat{\ell}}^s}{L}. \quad (24)$$

From (22) and (23) we thus have

$$x_{\hat{\ell}}^s = \left(\frac{1}{2} - \frac{\lambda}{\pi} \right) \hat{\ell}^2 + \left(\frac{1}{2} - \frac{2\lambda}{\pi} \right) \hat{\ell}. \quad (25)$$

We have checked these values via a direct independent numerical diagonalization of the transfer matrices for strips of width $L = 2, 4, 6, 8$.

Result (25) is in direct agreement with that obtained via conformal invariance arguments [5, 6]. Physically, these dimensions characterize the correlation of half-watermelon configurations, with the correlator along the surface decaying at criticality as

$$\langle \phi_{\hat{\ell}}(\mathbf{X}) \phi_{\hat{\ell}}(\mathbf{Y}) \rangle \sim |\mathbf{X} - \mathbf{Y}|^{-2x_{\hat{\ell}}^s} \quad (26)$$

where $\hat{\ell}$ self-avoiding walks are tied at their extremities \mathbf{X} and \mathbf{Y} located near the surface [6]. Thus $x_{\hat{\ell}}^s = (3\hat{\ell} + 2)\hat{\ell}/8$ for dilute polymers ($\lambda = \pi/8$), $x_{\hat{\ell}}^s = (\hat{\ell} - 2)\hat{\ell}/8$ for dense polymers ($\lambda = 3\pi/8$) and $x_{\hat{\ell}}^s = (\hat{\ell} - 1)\hat{\ell}/6$ at the Duplantier-Saleur θ -point [24] ($\lambda = \pi/3$).

Apart from the six-vertex model [18] and the present model, it appears that no other models have been solved in the present geometry, i.e. with free boundaries across a strip in the diagonal direction. It will be worthwhile seeking similar Bethe ansatz solutions of other lattice models. Later we hope to report on a similar treatment of the $O(n)$ model on the square lattice [25, 17, 26].

One of the authors (JS) is grateful for the hospitality shown to him by the Mathematics Department, Australian National University where this work was done. This work has been supported by the Australian Research Council.

References

- [1] de Gennes P G 1979 *Scaling Concepts in Polymer Physics* (Ithaca: Cornell University)
- [2] Cardy J L 1987 *Phase Transitions and Critical Phenomena* vol 11, ed C Domb and J L Lebowitz (London: Academic) p 55
- [3] Duplantier B 1989 *Phys. Rep.* **184** 229
- [4] Nienhuis B 1990 *Fundamental Problems in Statistical Mechanics* vol VII, ed H van Beijeren (Amsterdam: Elsevier) p 255
- [5] Cardy J L 1984 *Nucl. Phys. B* **240** 514
- [6] Duplantier B and Saleur H 1986 *Phys. Rev. Lett.* **57** 3179; 1987 *Nucl. Phys. B* **290** 291
- [7] De'Bell K and Lookman T 1993 *Rev. Mod. Phys.* **65** 87
- [8] Cardy J L 1984 *J. Phys. A: Math. Gen.* **17** L385
- [9] Domany E, Mukamel D, Nienhuis B and Schwimmer A 1981 *Nucl. Phys. B* **190** 279
- [10] Nienhuis B 1982 *Phys. Rev. Lett.* **49** 1062
- [11] Baxter R J 1986 *J. Phys. A: Math. Gen.* **19** 2821
- [12] Izergin A G and Korepin V E 1981 *Commun. Math. Phys.* **79** 303
- [13] Reshetikhin N Yu 1991 *J. Phys. A: Math. Gen.* **24** 2387
- [14] Vichirko V and Reshetikhin N Yu 1983 *Theor. Math. Phys.* **56** 260

- [15] Mezincescu L M and Nepomechie R I 1992 *Nucl. Phys. B* **372** 597
- [16] Tarasov V 1988 *Theor. Math. Phys.* **76** 184
- [17] Batchelor M T, Nienhuis B and Warnaar S O 1989 *Phys. Rev. Lett.* **62** 2425
Warnaar S O 1989 *Doctoraalscriptie* Rijksuniversiteit Leiden
- [18] Owczarek A L and Baxter R J 1989 *J. Phys. A: Math. Gen.* **22** 1141
- [19] Batchelor M T and Blöte H W J 1988 *Phys. Rev. Lett.* **61** 138
Suzuki J 1988 *J. Phys. Soc. Japan* **57** 2966
Batchelor M T and Blöte H W J 1989 *Phys. Rev. B* **39** 2391
- [20] Suzuki J, Nagao T and Wadati M 1992 *Int. J. Mod. Phys. B* **6** 1119
- [21] Baxter R J 1987 *J. Phys. A: Math. Gen.* **20** 5241
- [22] de Vega H J and Woynarovich F 1985 *Nucl. Phys. B* **251** 439
- [23] Blöte H W J, Cardy J L and Nightingale M P 1986 *Phys. Rev. Lett.* **56** 742
- [24] Duplantier B and Saleur H 1987 *Phys. Rev. Lett.* **59** 539
- [25] Nienhuis B 1990 *Int. J. Mod. Phys. B* **4** 929
- [26] Warnaar S O, Batchelor M T and Nienhuis B 1992 *J. Phys. A: Math. Gen.* **25** 3077